Author Manuscript

Author Manuscript

Author Manuscript

Author Manuscript

HHS Public Access

Author manuscript

J Immunol. Author manuscript; available in PMC 2015 October 27.

Published in final edited form as:

J Immunol. 2006 May 1; 176(9): 5426–5437.

A Role for the MutL Mismatch Repair Mlh3 Protein in Immunoglobulin Class Switch DNA Recombination and Somatic Hypermutation1

Xiaoping Wu[*], **Connie Y. Tsai**[*], **Marienida B. Patam**[*], **Hong Zan**[*], **Jessica P. Chen**[†], **Steve M. Lipkin**[†], and **Paolo Casali**[*,†,2]

[*]Center for Immunology, School of Medicine and School of Biological Sciences, University of California, Irvine, CA 92697

[†]Department of Medicine, School of Medicine and School of Biological Sciences, University of California, Irvine, CA 92697

Abstract

Class switch DNA recombination (CSR) and somatic hypermutation (SHM) are central to the maturation of the Ab response. Both processes involve DNA mismatch repair (MMR). MMR proteins are recruited to dU:dG mispairs generated by activation-induced cytidine deaminase-mediated deamination of dC residues, thereby promoting S-S region synapses and introduction of mismatches (mutations). The MutL homolog Mlh3 is the last complement of the mammalian set of MMR proteins. It is highly conserved in evolution and is essential to meiosis and microsatellite stability. We used the recently generated knockout *mlh3*$^{-/-}$ mice to address the role of Mlh3 in CSR and SHM. We found that Mlh3 deficiency alters both CSR and SHM. *mlh3*$^{-/-}$ B cells switched in vitro to IgG and IgA but displayed preferential targeting of the RGYW/WRCY (R = A or G, Y = C or T, W = A or T) motif by Sγ1 and Sγ3 breakpoints and introduced more insertions and fewer donor/acceptor microhomologies in Sμ-Sγ1 and Sμ-Sγ3 DNA junctions, as compared with *mlh3*$^{+/+}$ B cells. *mlh3*$^{-/-}$ mice showed only a slight decrease in the frequency of mutations in the intronic DNA downstream of the rearranged J_H4 gene. However, the residual mutations were altered in spectrum. They comprised a decreased proportion of mutations at dA/dT and showed preferential RGYW/WRCY targeting by mutations at dC/dG. Thus, the MMR Mlh3 protein plays a role in both CSR and SHM.

The maturation of Abs is underpinned by two genetic processes: class switch DNA recombination (CSR); and somatic hypermutation (SHM). By replacing the C region of the H chain with a downstream C_H region, CSR endows Abs with new biologic effector functions. By diversifying the binding strength of the surface receptor for Ag, SHM provides the structural substrate for selection by Ag of higher affinity mutants. CSR involves

---

[1]This work was supported by National Institutes of Health Grants AR 40908, AI 45011, and AI 60537 (to P.C.).

[2]Address correspondence and reprint requests to Professor Paolo Casali, Center for Immunology, 3028 Hewitt Hall, University of California, Irvine, CA 92657-4120. pcasali@uci.edu.

Disclosures

The authors have no financial conflict of interest.

Author Manuscript Author Manuscript Author Manuscript Author Manuscript

intrachromosomal deletional rearrangement between switch (S) regions. These lie upstream of each C_H region with the exception of Cδ and consist of highly repetitive G/C-rich sequences. Such repetitive sequences vary in different S regions. In the Sμ region, they consist of $((GAGCT)_n(GGGGT))$ repetitive units, where AGCT is the most common iteration of RGYW/ WRCY. During CSR, a composite junction between Sμ and a downstream S region is generated, and the intervening DNA is looped out as a circle. SHM preferentially targets the RGYW/ WRCY mutational hotspot and introduces point mutations with rare deletions or insertions into rearranged Ig *V(D)J* gene sequence, the human *Bcl-6* protooncogene in germline configuration, and the c-*Myc* protooncogene when translocated into the *Ig* locus, while sparing Ig C regions.

CSR entails the generation of double-strand DNA breaks (DSBs), which are obligatory intermediates in the process (1, 2) and may contribute to SHM as well (3–7). Both CSR and SHM require the intervention of activation-induced cytidine deaminase (AID) (8, 9), which preferentially deaminates dC within WRC, as shown in single-stranded DNA in vitro, to yield dU:dG mispairs in S and V regions (10, 11). In Ig V genes and S regions, WRC/GYW occur in most cases as part of the RGYW/WRCY consensus motif. Such dU:dG mispairs can be replicated over or processed by base excision repair, involving deglycosylation of dU by uracil DNA glycosylase (UNG) and abasic site excision by apurinic/apyrimidinic endonuclease (12, 13). dU:dG mispairs are also dealt with by the mismatch repair (MMR) machinery (12, 13). AID-independent generation of DSBs can also occur in S and V regions (6, 14–17). These DSBs may be processed by AID and MMR that would initiate repair processes leading to CSR and SHM (5, 6, 18, 19). Thus, MMR proteins are involved in resolving DNA lesions that underlie CSR and SHM.

MMR is one of the DNA repair pathways conserved from bacteria to humans. It contributes to maintain the integrity of the genome by correcting mismatched bases that arise through DNA replication errors and DNA damage. The genes of the MMR components were initially identified in *Escherichia coli* and designated *Mut* genes. Four *Mut* gene families are involved in MMR: MutS, MutL, MutH, and MutU. MutS first recognizes the mismatched DNA site, and recruits MutL, which in turn binds and activates the MutH endonuclease. The mismatched DNA oligonucleotide is then excised, and DNA is resynthesized correctly by DNA polymerase III (20). Five MutS (Msh2, Msh3, Msh4, Msh5, and Msh6) and four MutL (Mlh1, Mlh3, Pms1 (in which Pms is post-meiotic segregation), Pms2) homologs exist in mammals (21). The three MutS homologs, Msh2, Msh3, and Msh6, initiate MMR by forming Msh2-Msh6 and Msh2-Msh3 complexes at the site of nucleotide mispair. In a subsequent step, Mlh1-Pms2, Mlh1-Mlh3 heterodimers of MutL homologs, as well as exonuclease ExoI, are recruited and ultimately the mismatch-containing DNA is excised. A new stretch of the DNA strand is then resynthesized by the high fidelity polymerase δ (patch repair) (22–24) or error-prone translesion DNA polymerases when new DNA synthesis occurs as part of SHM and perhaps CSR (5, 25). The remaining two MutS homologs, Msh4 and Msh5, are specifically involved in meiosis and do not appear to play a role in somatic DNA repair process (26–29). The fourth mammalian MutL homolog, Pms1, plays a marginal role in MMR (30).

Author Manuscript Author Manuscript Author Manuscript Author Manuscript

MMR proteins have been linked directly to CSR and SHM (Table I). Lack of Msh2 decreased the frequency of CSR (31, 32, 47) and SHM with a reduction in dA/dT mutations (35). Msh6 but not Msh3 deficiency reduced CSR and SHM (38, 39). Like their Msh2-deficient counterparts, Msh6-deficient mice showed fewer somatic mutations at dA/dT in both Ig V and S regions. The Msh2/ Msh6 complex would bind to transcribed S regions, promote S-S synapsis (48), and stimulate the activity of DNA polymerase η, thereby suggesting a role of Msh2 and/or Msh6 in SHM at dA/dT residues (49). Deficiencies in the two MutL homologs Mlh1 and Pms2 also reduced CSR and SHM (32, 41–44) and altered the sequence of S-S junctions (33, 34, 43), but their effect on the pattern of SHM appear to be controversial (39–44). In Msh2/Mlh1-deficient B cells, CSR frequency was reduced in a manner reminiscent of single Msh2- or Mlh1-deficient B cells. However, the junctional Sμ-Sγ3 sequences resembled those found in Mlh1- but not Msh2-deficient B cells (28, 33, 34).

Mlh3 is the last characterized mammalian MMR protein and the last element to complete the set of mammalian MMR homologs (50, 51). Mlh3 is highly conserved in evolution and is essential for meiosis, but its role in mammalian MMR is not fully understood. Here, we have addressed the role of Mlh3 in CSR and SHM by using the recently generated knockout *mlh3*$^{-/-}$ mice (52). The contribution of Mlh3 to S-S DNA recombination was investigated by analyzing the surface Ig expression of splenic B cells stimulated by LPS and cytokines and the composition of the Sμ-Sγ1 and Sμ-Sγ3 DNA junctions and the locations of S region breakpoints with respect to RGYW/WRCY in the switched B cells. The contribution of Mlh3 to SHM was addressed by analyzing the frequency and pattern of the unselected mutations in the intronic DNA region downstream of the rearranged $V_HJ558DJ_H4$ gene segment.

Materials and Methods

Mlh3-deficient mice

The *mlh3*$^{-/-}$ mice used in these studies were created by gene targeting to delete exon 1 and exon 2 of the *mlh3* gene. This was accomplished by subcloning a genomic 3.6-kb fragment containing exon 1, exon 2, and the 5'-flanking sequence of the *Mlh3* gene derived from a 129 Sv/Ev phage library into the *NotI* site of pNT loxP vector and a genomic 6.3-kb fragment of the *Mlh3* intron into the *Eco*RI site (50). The targeting vector was linearized and electroporated into 129 Sv/Ev embryonic stem cells which were selected in neomycin to yield resistant colonies used for the generation of *mlh3*$^{-/-}$ mice. All mice used in this study were exposed only to environment Ags. *mlh3*$^{-/-}$ and *mlh3*$^{+/+}$ 129 Sv/Ev mice were bred in the vivarium of the University of California (Irvine, CA). All experiment protocols were approved by the Institutional Animal Care and Use Committee of the University of California.

Class switch DNA recombination

B cells are isolated from RBC-depleted splenocytes of mice with the B cell enrichment kit (StemCell Technologies) and were cultured at 10^6 cell/ml in 10% FCS-RPMI with 0.05 mM 2-ME. Cells were stimulated with LPS (10 μg/ml) from *E. coli* (serotype 055:B5; Sigma-Aldrich) and with or without 1) recombinant murine (rm) IL-4 (2 ng/ml; R&D Systems) for

Author Manuscript Author Manuscript Author Manuscript Author Manuscript

CSR to IgG or 2) human TGF-β (2 ng/ml), rmIL-4 (2 ng/ml), and rmIL-5 (5 ng/ml; R&D Systems) and anti-δ mAb-dextran (3 ng/ml; provided by C. M. Snapper, Uniformed Services University of the Health Sciences, Bethesda, MD) for CSR to IgA. Cells were collected on day 5 for FACS analysis of surface Ig expression.

FACS analysis

In vitro-stimulated B cells were harvested after culture for 5 days and stained with anti-mouse IgG1 (clone A85-1)-, anti-mouse IgG3 (clone R40–82)-, or anti-mouse IgG2b (clone R12-3)-FITC rat mAb and PE-conjugated anti-mouse CD45R (B220) (RA3–6B2) rat mAb (BD Biosciences). Cells were fixed with 1% paraformaldehyde in PBS and analyzed with a FACSCalibur flow cytometer (BD Biosciences).

S-S junctions

Genomic DNA was prepared from B cells cultured for 5 days after stimulation with LPS without or with rmIL-4. Junctional Sμ-Sγ3 and Sμ-Sγ1 DNA were amplified using two sequential rounds of specific PCR involving the following nested primers (43): aactctccagccacagtaatgacc (Sm1– 4942); ctactgagttcctgtgcttg (Sg3); ctgtaacctacccaggagacc (Sg1); acgctc gagaaggccagcctcataaagct (Sm2–4972); ccggaattcttgacctggtaccctagc (Sg3-NS); and gtcgaattcccccatcctgtcacctata (Sg1-NS). The first and second rounds of PCR were performed at 94°C for 40 s, 55°C for 40 s, 72°C for 2 min, 30 cycles. PCR DNA products were purified using Qiaquick PCR purification kit (Qiagen) and cloned into Zero Blunt TOPO vector (Invitrogen) for sequencing. Sequence alignment was done by comparing the sequences of PCR products with Sμ, Sγ1, and Sγ3 genomic sequences with the use of National Center for Biotechnology Information (NCBI) blast (www.ncbi.nih.gov/BLAST).

Somatic hypermutation

Peyer's patches were prepared from 8- to 12-wk-old *mlh3*$^{+/+}$ and *mlh3*$^{-/-}$ mice. Cells from the Peyer's patches were stained with PE-conjugated anti-mouse B220 rat mAb (BD Biosciences) and FITC-conjugated peanut agglutinin (PNA; E-Y Laboratories). Germinal center B220^{+} NA^{high} cells were sorted in a high output Moflo cell sorter (Cytomation). The intronic region downstream of rearranged Ig *VHDJ$_H$4* gene segments was amplified from genomic DNA with the use of primers specific for FR3 of the *V$_H$J558* gene and downstream of the *J$_H$4* gene segment. The primer sequences were gcctgacatctgaggactctgc and tgagaccgaggctagatgcc. The PCR-amplified DNA were cloned into the Zero Blunt TOPO cloning kit and sequenced.

DNA polymerase ι genotyping

To verify that the gene sequence of polymerase ι, which is a null mutant in all 129 mice examined (53), is identical in *mlh3*$^{-/-}$ and *mlh3*$^{+/+}$ mice, we analyzed the 410-bp DNA sequence encompassing exon 2 and containing the (Ser 27) TCG→TAG (amber) stop codon mutation characteristic of this polymerase gene in 129 mice. This genomic DNA was amplified from *mlh3*$^{+/+}$ and *mlh3*$^{-/-}$ spleen B cells with the 5'-ttaaagcaggactgaagacc-3' and 5'-cggttgaagctaattgctaa-3' primers. PCR was performed at 94°C for 30 s, 55°C for 30 s, 72°C for 30 min, 40 cycles. The amplified DNA was cloned into the Zero Blunt TOPO

Author Manuscript Author Manuscript Author Manuscript Author Manuscript

cloning kit and sequenced. The exon 2 Ser 27 stop codon TAG mutation was identified in both *mlh3*$^{+/+}$ and *mlh3*$^{-/-}$ 129 Sv/Ev mice.

Somatic point mutations in mouse mlh3$^{-/-}$ *fibroblasts*

Mouse embryonic fibroblasts (MEF) were cultured in 15-cm petri dishes in DMEM containing 15% FCS and 1 mM ouabain until mutant colonies developed after 8–10 days. After fixation with ethanol and staining with 10% methylene blue, the ouabain-resistant colonies were counted. The mutation rate was determined as the number of mutant colonies per total plated cells per cell generations (30). Three MEF cell lines from three different embryos were tested for either *mlh3*$^{-/-}$ or *mlh3*$^{+/+}$ genotype.

Cell proliferation and cell cycle analysis

B cells were isolated from RBC-depleted splenocytes of mice with a B cell enrichment kit (StemCell Technologies). Cells were stimulated with LPS (10 μg/ml; Sigma-Aldrich) and collected on day 3. After fixation in 70% ethanol overnight, cells were stained with 50 μg/ml propidium iodide (PI) and analyzed by FACSCalibur. For CFSE staining, fresh isolated B cells were stained with 5 μg/ml CFSE at 37°C for 10 min. After washing, cells were cultured and stimulated with LPS and collected on day 3 for FACS analysis. For in vivo BrdU incorporation, mice were immunized with 1×10^8 SRBC 1 wk before BrdU i.p. injection. Two 1-mg doses of BrdU were given to mice at 12-h intervals; 3 h after the second BrdU injection, mice were sacrificed to prepare spleen cells. The spleen cells were stained with PE-conjugated anti-B220, FITC-conjugated PNA, and APC-conjugated anti-BrdU (BD Biosciences) for FACS analysis.

Statistical analysis

Differences in numbers of microhomologies in Sμ-Sγ1 and Sμ-Sγ3 junctions between in vitro-stimulated *mlh3*$^{+/+}$ and *mlh3*$^{-/-}$ B cells was analyzed with the paired *t* test. The χ^2 test was used to analyze the differences in the distributions of S-region breakpoints at GAGCT, GGGGT, RGYW/ WRCY, WRC/GYW; and AGCT, the distribution of mutations at RGYW/ WRCY and WRC/GYW; or percentages of mutations at dA, dC, dG, and dT between *mlh3*$^{+/+}$ and *mlh3*$^{-/-}$ B cells or mice groups. *p* values <0.05 were considered to be statistically significant. Statistically difference in the mutation frequencies between genomic DNA of *mlh3*$^{-/-}$ and *mlh3*$^{+/+}$ cell lines were tested by the method of Equality of Two Binomial Proportions.

Results

Altered junctional Sμ-Sγ DNA microhomologies and insertions in Mlh3-deficient B cells

To investigate the role of Mlh3 in CSR, we induced CSR to IgG1 by LPS and IL-4, to IgG3 and IgG2b by LPS, and to IgA by LPS plus TGF-β, IL-4, IL-5, and anti-δ mAb-dextran in B cells from *mlh3*$^{-/-}$ mice and their *mlh3*$^{+/+}$ counterparts. *mlh3*$^{-/-}$ B cells were competent in switching to all secondary isotypes examined, as shown by the comparable levels of surface B cell secondary isotypes (Fig. 1). To further address the role of Mlh3 in CSR, we sequenced the recombined Sμ-Sγ1 and Sμ-Sγ3 DNA junctions of in vitro-stimulated B cells and compared them with the respective Sμ and Sγ genomic templates to determine: 1) the

Author Manuscript Author Manuscript Author Manuscript Author Manuscript

degree of putative overlap (microhomology) of the upstream Sμ and downstream Sγ1 or Sγ3 regions; and 2) the frequency of inserted un-templated nucleotides between the upstream Sμ and downstream Sγ1 or Sγ3 regions (insertions). Microhomologies and insertions accompany CSR. The Sμ-Sγ1 and Sμ-Sγ3 junctional DNAs were amplified with a specific PCR involving a forward primer encompassing a region 500 bp 5' of the highly repetitive $((GAGCT)_n(GGGGT))$ Sμ region and a reverse primer encompassing a region 1000 bp 3' of the tandem repeats of Sγ1 or 700 bp 3' of the tandem repeats of Sγ3. Analysis of 44 unique Sμ-Sγ1 and 44 unique Sμ-Sγ3 sequences in B cells from 5 *mlh3*$^{-/-}$ mice and 5 *mlh3*$^{+/+}$ littermates showed that the *mlh3*$^{-/-}$ B cells displayed reduced numbers of Sμ-Sγ1 (15 or 34% vs 27 or 61%; $p < 0.033$) and Sμ-Sγ3 (16 or 36% vs 33 or 75%; $p < 0.034$) junctional sequences entailing ≥1 nucleotide(s) microhomologies (Figs. 2 and 3). The average length of the microhomologies in Sμ-Sγ1 DNA of *mlh3*$^{-/-}$ B cells was 2.0 nucleotides as compared with 2.4 in *mlh3*$^{+/+}$ B cells; in Sμ-Sγ3 DNA of *mlh3*$^{-/-}$ B cells, it was 1.9 nucleotides, as compared with 2.9 in *mlh3*$^{+/+}$ B cells. The fewer number of junctions displaying S-S region overlaps and the reduced average length of the overlaps in S-S DNA in *mlh3*$^{-/-}$ B cells as compared with *mlh3*$^{+/+}$ B cells were complemented by more sequences entailing blunt junctions or insertions in the Sμ-Sγ1 and Sμ-Sγ3 junctions (Table II). Sμ-Sγ1 DNA from *mlh3*$^{-/-}$ B cells included 20 (45%) and 9 (21%) sequences entailing blunt junctions and insertions, respectively, as compared with 15 (34%) and 2 (5%) in *mlh3*$^{+/+}$ B cells ($p < 0.048$). Sμ-Sγ3 DNA from *mlh3*$^{-/-}$ B cells included 16 (36%) and 12 (27%) sequences entailing blunt junctions and insertions, respectively, as compared with 8 (18%) and 3 (7%) in *mlh3*$^{+/+}$ B cells ($p < 0.016$). Thus, Mlh3 deficiency gave rise to altered Sμ-Sγ DNA sequences involving significantly decreased microhomologies and significantly increased blunt junctions and insertions.

Altered Sγ region breakpoints in Mlh3-deficient B cells

The altered pattern of S-S junctions in *mlh3*$^{-/-}$ B cells prompted us to ask whether the distribution of S DNA breakpoints in these B cells was different from those of *mlh3*$^{+/+}$ B cells. Because of the preferential targeting of the RGYW/WRCY hotspot by SHM and DSBs in the Ig V(D)J DNA (6), we examined RGYW/WRCY for the presence of S region breakpoints. We also analyzed the distribution of S region breakpoints in the 16 iterations of RGYW/ WRCY, among which the AGCT represents the most frequent iteration in mouse and human S regions (H. Zan, manuscript in preparation). In the S region sequences considered here, AGCT accounts for 28, 37, and 19% of the 16 RGYW/WRCY iterations in Sμ, Sγ1, and Sγ3, respectively. When an S-S junctions is blunt or contains insertions, the location of the breakpoints is readily determined. When donor-acceptor microhomologies are present, the exact location of breakpoints can be ambiguous, namely, the breakpoint of either Sμ or Sγ could have occurred 5' of, 3' of, or within the microhomology.

Analysis of all putative breakpoints in the Sμ-Sγ1 and Sμ-Sγ3 DNA junctions showed that RGYW/WRCY, including the preponderant AGCT iteration, was preferentially targeted by Sγ1 and Sγ3 region breakpoints in *mlh3*$^{-/-}$ B cells (Fig. 4). In *mlh3*$^{-/-}$ B cells, 57% of the Sγ1 breakpoints fell within RGYW/WRCY, which accounts for only 36% of all the nucleotides of this S region, as compared with 34% in *mlh3*$^{+/+}$ B cells ($p < 0.05$). Preferential RGYW/WRCY targeting by breakpoints also occurred in the Sγ3 region. In

Author Manuscript Author Manuscript Author Manuscript Author Manuscript

mlh3$^{-/-}$ B cells, 55% of the Sγ3 breakpoints fell within RGYW/WRCY, which accounts for 42% of all the nucleotides in this region, as compared with 30% in *mlh3*$^{+/+}$ B cells ($p < 0.05$; Table III). The increased targeting of RGYW/WRCY by Sγ1 and Sγ3 breakpoints in *mlh3*$^{-/-}$ B cells was the result of the increased targeting of AGCT as well as other RGYW/WRCY iterations by Sγ1 and Sγ3 breakpoints. However, in both *mlh3*$^{-/-}$ and *mlh3*$^{+/+}$ B cells, AGCT was predominantly targeted by Sγ1 and Sγ3 breakpoints, as compared with other RGYW/WRCY iterations; 83 and 67% RGYW/WRCY breakpoints targeted AGCT in *mlh3*$^{-/-}$ or *mlh3*$^{+/+}$ B cells, respectively. Preferential RGYW/WRCY targeting could not be detected in Sμ, in either Sμ-Sγ1 or Sμ-Sγ3 DNA junctions. In *mlh3*$^{-/-}$ B cells, RGYW/WRCY, which accounts for 44% of all the Sμ region nucleotides, was targeted by 55% of all Sμ reakpoints in Sμ-Sγ1 junctions and 43% of all Sμ breakpoints in Sμ-Sγ3 junctions, as compared with 59 and 50%, respectively, in *mlh3*$^{+/+}$ B cells (Table III). Thus, Mlh3 deficiency resulted in preferential breakpoint targeting of RGYW/WRCY, particularly AGCT, in Sγ1 and Sγ3 regions. Analysis of the distribution of S region breakpoints with respect to WRC/GYW yielded a pattern comparable with that of RGYW/WRCY; i.e., Sγ1 and Sγ3 region breakpoints preferentially targeted the WRC/GYW AID hotspot in *mlh3*$^{-/-}$ but not *mlh3*$^{+/+}$ B cells (data not shown).

Altered Sμ-Sγ microhomologies associate with altered S region breakpoints in Mlh3-deficient B cells

Because of the decreased number of microhomologies in Sμ-Sγ1 and Sμ-Sγ3 junctions and the preferential targeting of RGYW/ WRCY by Sγ1 and Sγ3 breakpoints, we asked whether S-S junctions within and outside RGYW/WRCY in *mlh3*$^{-/-}$ B cells were different from those in *mlh3*$^{+/+}$ B cells; in other words, whether the S-S junctions entailing microhomologies, blunt junctions, and insertions differed with respect to RGYW/WRCY targeting. To this end, we examined the locations of breakpoints entailing microhomologies of ≥1 nucleotide, blunt junctions, and insertions in Sγ1, Sγ3, and Sμ regions and found it to be significantly altered in *mlh3*$^{-/-}$ B cells. In the Sγ1 region of these cells, the breakpoints outside RGYW/WRCY entailing microhomologies and nonmicrohomologies were 21 and 79%, as compared with 55 and 45%, respectively, in *mlh3*$^{+/+}$ B cells ($p < 0.05$; Table IV); in the Sγ3 region, the breakpoints outside RGYW/WRCY entailing microhomologies and nonmicrohomologies were 25 and 75% in *mlh3*$^{-/-}$ B cells, as compared with 71 and 29%, respectively, in *mlh3*$^{+/+}$ B cells ($p < 0.05$). Thus, the decreased junctional Sμ-Sγ1, and Sμ-Sγ3 microhomologies in *mlh3*$^{-/-}$ B cells were associated with decreased Sγ1 and Sγ3 breakpoints outside RGYW/ WRCY. Similar features were also displayed by Sμ breakpoints in both Sμ-Sγ1 and Sμ-Sγ3 junctional DNA of *mlh3*$^{-/-}$ B cells ($p < 0.05$). Thus, the significantly decreased frequency of Sμ-Sγ1 recombinations involving microhomologies in *mlh3*$^{-/-}$ B cells associated with a decreased targeting of residues outside RGYW/ WRCY by breakpoints in Sμ, Sγ1, and Sγ3 regions.

Altered SHM in Mlh3-deficient mice

Msh2 (35, 36) or Msh6 deficiency (38–40) increases mutations at dC/dG with a preponderance of transitions and preferential targeting of RGYW/WRCY. Mlh1 or Pms2 deficiency decreases mutations, but its effect on the nature of SHM is discordant (42, 43). To determine whether Mlh3 is involved in SHM, B220^{+}PNA^{high} cells were sorted from

Author Manuscript Author Manuscript Author Manuscript Author Manuscript

Peyer's patches of *mlh3*$^{-/-}$ and *mlh3*$^{+/+}$ litter-mates to amplify and sequence the intronic DNA lying 400 bp downstream of rearranged V_HDJ_H4 genes (J_H4 intronic DNA) (54). *mlh3*$^{-/-}$ and *mlh3*$^{+/+}$ mice displayed comparable frequencies of V_HDJ_H rearrangements involving J_H4. This intronic DNA is targeted by SHM but does not undergo selection by Ag during affinity maturation. Clonal uniqueness was determined by the sequences of different V_HDJ_H4 rearrangements upstream the J_H4 intronic region. This showed a slightly decreased frequency of mutations in 3 *mlh3*$^{-/-}$ mice as compared with their *mlh3*$^{+/+}$ littermates (Fig. 5, *A* and *B*). However, *mlh3*$^{-/-}$ mice displayed a significantly increased proportion of mutations at dC/dG (60.2% vs 41.5%, $p < 0.05$) (Fig. 5, *C* and *D*). In addition, in *mlh3*$^{-/-}$ mice, dG was the most frequently mutated residue, with 42.4% of the overall mutations targeting dG, as compared with 29.6% in *mlh3*$^{+/+}$ mice ($p < 0.05$). dA was the most frequently mutated residue in *mlh3*$^{+/+}$ mice, with 41.5% of the overall mutations targeting dA, as compared with 23.8% in *mlh3*$^{-/-}$ mice ($p < 0.05$). In *mlh3*$^{-/-}$ mice, transitions in mutations at both dC/dG and dA/dT were decreased, with those at dA/dT significantly decreased ($p < 0.01$), as compared with *mlh3*$^{+/+}$ mice. In addition, the mutations at dC/dG targeted the RGYW/WRCY hotspot at a significantly higher frequency than in *mlh3*$^{+/+}$ mice. There are a total of 21 RGYW/WRCY motifs in the J_H4 intronic region, accounting for 21% of this sequence. In *mlh3*$^{-/-}$ mice, 46% of the mutations at dC/dG targeted RGYW/WRCY, as compared with 28% in *mlh3*$^{+/+}$ mice ($p < 0.05$), while mutations at dA/dT residues were not significantly different with respect to RGYW/WRCY targeting (Table V). Thus, overall, Mlh3 deficiency resulted in a significant alteration of SHM entailing a preferential targeting of dC/dG, particularly dC/dG at RGYW/WRCY, and an increased transversion mutations at dA/dT.

Mlh3 deficiency correlates with an increased mutation rate at non-*Ig* loci

The altered pattern of somatic mutations in *mlh3*$^{-/-}$ mice suggested a role of Mlh3 in the patch repair process underlying SHM. To investigate whether the altered SHM found in those *mlh3*$^{-/-}$ mice reflected a more general function of this MMR MutL protein, we examined the genomic DNA mutation rate in Mlh3-deficient MEF using a colony formation assay that measures the acquisition of ouabain resistance (30). In this assay, increased DNA mutations result in increased resistance to ouabain, i.e., outgrowth of colony-forming cells. After 9 days of culture in ouabain-containing medium, the DNA mutation rate giving rise to ouabain resistance in *mlh3*$^{-/-}$ fibroblasts was significantly higher than in *mlh3*$^{+/+}$ fibroblasts (5.8×10^{-7} vs 1.5×10^{-7} mutation/cell/division, $p < 0.01$). Thus, Mlh3 plays a role in repairing spontaneously arising mutations in genomic DNA of mouse cells.

Mlh3-deficient B cells show no defect in cell cycle and proliferation

CSR frequency may be associated with cell division (55). To rule out the possibility that the altered modalities of CSR and SHM in *mlh3*$^{-/-}$ B cells were not a reflection of altered rates of cell division and cell death or an alteration of the proportion of germinal center B cells, we analyzed *mlh3*$^{-/-}$ B cells for cell cycle, proliferation and ratio of germinal center B cells. *mlh3*$^{-/-}$ B cells stimulated in vitro exhibited comparable cell cycle, as measured by PI incorporation, and comparable cell division, as measured by CFSE content, to the *mlh3*$^{+/+}$ B cells (Fig. 6). In *mlh3*$^{-/-}$ mice, in vivo B cell proliferation, as measured by BrdU incorporation, was also comparable with that in *mlh3*$^{+/+}$ mice. Thus, the alterations in CSR

Author Manuscript Author Manuscript Author Manuscript Author Manuscript

and SHM found in *mlh3*$^{-/-}$ B cells do not merely reflect an altered pattern of B cell cycle and/or proliferation.

Discussion

We have shown here that in the absence of Mlh3, CSR exhibits an altered pattern of Sμ-Sγ1 and Sμ-Sγ3 junctions with a decrease in microhomologies, increased insertions and blunt junctions, and altered distribution of breakpoints in Sγ1 and Sγ3 regions. Further, in the absence of Mlh3, SHM preferentially targets dC/dG. These findings point at Mlh3 as an important element in the MMR events that underlie CSR and SHM and unveil a new role for Mlh3 in DNA repair, in addition to the contribution of this MutL protein to DNA microsatellite stability (50).

The human genome project has shown that there are nine homologs of *E. coli MutS* and *MutL* genes encoded in mammals (www.ncbi.nlm.nih.gov). Mouse models for all nine have been created (26, 27, 29, 30, 52, 57– 61). Mammalian Mlh3, the last characterized MutL homolog and complement of the MMR set of proteins, is essential for meiosis. Mlh3 deficiency causes increased frame shift mutations, defects in DNA damage-induced apoptosis, and gastrointestinal cancer susceptibility (62). Mlh3 and Pms2 bind competitively to the same Mlh1 domain to form two different functional MutL heterodimers (51), implying that the molecular ratio of Mlh3 to Pms2 determines the formation of different MutL heterodimers and, possibly, the efficacy of CSR. The different impact of Pms2 deficiency, which significantly reduces the frequency of CSR, and Mlh3 deficiency, which does not change the frequency of CSR, suggests that these two MutL proteins confer different functions to the respective Pms2-Mlh1 and Mlh3-Mlh1 het-erodimers. Likewise, in male meiosis, whereas Pms2 plays a critical role in the pachynema stage, Mlh3 performs an essential function in the diplonema stage (52).

The reduced degree of microhomology and increased number of insertions in the Sμ-Sγ1 and Sμ-Sγ3 junctions in Mlh3-deficient B cells are evocative of those in Msh2-deficient B cells (33, 34) but contrast with the high degree of microhomology in S-S junctions of Pms2- or Mlh1-deficient B cells (33, 43). Microhomologies would result from the synapsis of complementary S region DSB staggered ends, whereas blunt junctions and insertions would result mainly from the synapsis of S region DSB blunt ends (18). Insertions could result from imprecise joining of either DSB end. Both the decreased S-S junction microhomology, as in Msh2 deficiency (33, 34), and increased S-S junction microhomology, as in Mlh1 or Pms2 deficiency (33, 34), have been associated with decreased CSR frequency in vitro (31, 32, 43). The seemingly unchanged CSR frequency in Mlh3-deficient B cells suggests that both microhomology-involving and non-microhomology-involving S-S synapsis are “valid” events for CSR.

How Mlh3 contributes to microhomology-mediated CSR remains to be determined. Mlh3 can play a direct role in microhomology-mediated S-S recombination or can dampen Pms2 function, which plays a role in non-microhomology-mediated S-S recombination. These two possibilities are not mutually exclusive. Interestingly, yeast Mlh3 associates with Msh3 to suppress insertions/deletions (63), and Msh3-deficient B cells showed a significant increase

Author Manuscript Author Manuscript Author Manuscript Author Manuscript

in insertions at S-S junctions (38, 39), a feature partially observed in our Mlh3-deficient B cells, suggesting that Mlh3 can associate with Msh3 in the rejoining of S-region DNA. These results also parallel the phenotype of Mlh3 deficiency in repetitive sequence (microsatellite) repair, which shows a bias toward repair of deletions but not insertions (61). Deficiencies in other DNA repair proteins also alter the patterns of S-S junctions. Patients with ataxia-telangiectasia (Atm deficiency) (64), at axia-telangiectasia-like disorder (Mre11 deficiency) (65), and Nijmegen breakage syndrome (Nbs-1 deficiency) (65) show increased microhomology at S-S junctions, as do Atm-deficient mice (66, 67), suggesting that these proteins, together with Mlh1 and Pms2, play an important role in mediating S-S recombination not involving microhomologies. Thus, Mlh3 may, in association with Msh2-Msh3, suppress the introductions of insertions into S-S junctions, while promoting S-S resolution events that entails introduction of microhomologies.

Like in Msh6-deficiency, in which Sγ3 but not Sμ breakpoints preferentially target RGYW/WRCY (38), Mlh3 deficiency resulted in preferential targeting of breakpoints to RGYW/WRCY in both Sγ1 and Sγ3 regions (Table III). This could reflect the role of Mlh3 in facilitating S-S recombination occurring outside RGYW/ WRCY. The normal frequency of CSR in the absence of Mlh3 suggests that Mlh3 is not essential in the initial steps of CSR. Sμ tandem repeats that are rich in RGYW/WRCY undergo breakage and mediate CSR independently of Msh2. In contrast, DNA breakage in sequences flanking the Sμ tandem repeats requires Msh2 to allow recombinational joining and CSR to unfold (68, 69), implicating a more significant role of MMR proteins in S-S DNA recombination events involving sequences with scarcity of RGYW/ WRCY (68). Thus, Mlh3 deficiency shifts the Sy breakpoints of Sμ-Sγ to RGYW/WRCY, implicating a significantly role of Mlh3 in facilitating S-S recombination events outside RGYW/WRCY. Dissection of the distribution of Sμ, Sγ1, and Sγ3 region breakpoints in different RGYW/WRCY iterations showed that AGCT, an evolutionarily conserved motif for CSR (70), is the most frequently occurring iteration and is most frequently targeted by S-region breakpoints in both *mlh3*$^{-/-}$ and *mlh3*$^{+/+}$ B cells.

Our findings show that Mlh3 contributes to both CSR and SHM. Deficiency in either Pms2 (28, 32, 33, 41, 44–46) or Mlh1 (32, 41–43) resulted in impairment of CSR but affected SHM inconsistently. As shown by analysis of the J_H4 intronic region of B220^{+}PNA^{high} germinal center B cells, the absence of Mlh3 significantly altered SHM. Mutations at dA/dT residues were markedly diminished ($p < 0.05$), and mutations at dC/dG preferentially targeted the RGYW/WRCY mutational hotspot ($p < 0.05$) in *mlh3*$^{-/-}$ as compared with *mlh3*$^{+/+}$ mice (Table V). These features are reminiscent of those of Msh2 (35)-, Msh6 (38–40)-, and ExoI-deficient mice (71), which are consistent with a two-phase process in CSR and SHM. Phase 1 entails dC deamination by AID to yield a dU:dG mismatch. This can be replicated over leading to a dG→dA transition or can be removed by UNG. DNA synthesis opposite the resultant abasic site by translesion polymerases will lead to introduction of a dC→dT transition or dC→dA and dG transversions (phase 1B). It can also be resolved by mutagenic patch repair, which is central to phase 2, in which dU:dG mismatches are dealt with by the MMR machinery. Indeed, absence of Msh2 results in ablation of phase 2 and diminished mutations at dA/dT without transversion bias (12, 35). The contribution of Mlh3

Author Manuscript Author Manuscript Author Manuscript Author Manuscript

to SHM likely reflects the role of Mlh3 in genomic DNA repair. Indeed, as we have shown, lack of Mlh3 gives rise to a higher genomic DNA mutation rate in non-B cells, further strengthening a role of the this MutL protein in the DNA repair process specifically underpinning SHM, as *mlh3*$^{-/-}$ B cells proliferate and undergo normal cell cycle in vitro and in vivo (Fig. 6). Thus, the altered S-S junctional sequences and the pattern of SHM in *mlh3*$^{-/-}$ B cells reflected the intrinsic participation of Mlh3 in the molecular process of CSR and SHM.

The mutagenic Phase 2 patch repair contributes to mutations at dA/dT residues and has been suggested to involve DNA polymerase η (37, 72–74), which would be recruited by the Msh2-Msh6 complex (49). The significant decrease in dA/dT mutations in *mlh3*$^{-/-}$ mice suggests that Mlh3, through complexing with Msh2-Msh6, is also involved in recruiting polymerase 17 to introduce mutations at dA/dT. In addition to polymerase 17, other error-prone translesion DNA polymerases may be recruited by and work in concert with Mlh3 and other MMR proteins in SHM, including polymerases ι (75) and θ (76). These can insert mismatches, which are then extended by polymerases θ itself or polymerase ζ (76, 77). Like polymerase η- or Msh6-deficient mice (28, 37, 38, 72, 74), Mlh3-deficient mice show preferential transversion mutations at dA/dT residues. The altered pattern of mutations in Mlh3-deficient mice as compared with Mlh1- and Pms2-deficient mice suggests that Mlh3 can function independently of Mlh1 in SHM. Likewise, in male meiosis, Mlh3 binds to germ cell chromosomal chiasmata sites in the diplonema stage independently of Mlh1 (52).

In conclusion, the significant alteration of S-S junctions in the absence of Mlh3 suggests that Mlh3 contributes to the creation and/or stabilization of microhomologies between the upstream Sμ ends of and downstream DNA ends of Sγ1 or Sγ3. This function contrasts with that of Pms2, which contributes to non-microhomol-ogy-mediated S-S recombination (43). The profound alteration of the pattern of SHM in *mlh3*$^{-/-}$ mice indicates a role of Mlh3 in the patch repair events leading to SHM and suggests that Mlh3 plays a significant role in targeting mutations at dA/dT, at which the transitional mutations are most affected. Further studies will address the association of Mlh3 with the error-prone DNA polymerases that introduce mutations at dA/dT, particularly transition mutations, and other MMR proteins that associate with Mlh3 in the process of CSR and SHM.

Acknowledgments

We thank Dr. Clifford M. Snapper for mouse anti-δ mAb-dextran and Mr. Junli Feng for excellent technical assistance.

Abbreviations used in this paper

AID	activation-induced cytidine deaminase
CSR	class switch DNA recombination
DSB	double-strand DNA breaks
Mlh3	MutL homolog 3
MMR	mismatch repair

Author Manuscript Author Manuscript Author Manuscript Author Manuscript

PI	propidium iodide
Pms2	postmeiotic segregation 2
SHM	somatic hypermutation
UNG	uracil DNA glycosylase
rm	recom-binant murine
PNA	peanut agglutinin
MEF	mouse embryonic fibroblasts
Atm	ataxia-telangiectasia

References

1. Chaudhuri J, Alt FW. Class-switch recombination: interplay of transcription, DNA deamination and DNA repair. Nat. Rev. Immunol. 2004; 4:541–552. [PubMed: 15229473]
2. Honjo T, Muramatsu M, Fagarasan S. AID: how does it aid antibody diversity? Immunity. 2004; 20:659–668. [PubMed: 15189732]
3. Bross L, Fukita Y, McBlane F, C D, Rajewsky K, Jacobs H. DNA double-strand breaks in immunoglobulin genes undergoing somatic hypermuta-tion. Immunity. 2000; 13:589–597. [PubMed: 11114372]
4. Papavasiliou FN, Schatz DG. Cell-cycle-regulated DNA double-stranded breaks in somatic hypermutation of immunoglobulin genes. Nature. 2000; 408:216–221. [PubMed: 11089977]
5. Wu X, Feng J, Komori A, Kim EC, Zan H, Casali P. Immunoglobulin somatic hypermutation: double-strand DNA breaks, AID and error-prone DNA repair. J. Clin. Immunol. 2003; 23:235–246. [PubMed: 12959216]
6. Zan H, Wu X, Komori A, Holloman WK, Casali P. AID-depen-dent generation of resected double-strand DNA breaks and recruitment of Rad52/ Rad51 in somatic hypermutation. Immunity. 2003; 18:727–738. [PubMed: 12818155]
7. Xu Z, Fulop Z, Zhong Y, Evinger A, Zan H, Casali P. DNA and repair in immunoglobulin class switch recombination and somatic hypermutation. Ann. NY Acad. Sci. 2005; 1050:146–162. [PubMed: 16014529]
8. Muramatsu M, Kinoshita K, Fagarasan S, Yamada S, Shinkai Y, Honjo T. Class switch recombination and hypermutation require activation-induced cytidine deaminase (AID), a potential RNA editing enzyme. Cell. 2000; 102:553–563. [PubMed: 11007474]
9. Revy P, Muto T, Levy Y, Geissmann F, Plebani A, Sanal O, Catalan N, Forveille M, Dufourcq-Labelouse R, Gennery A, et al. Activation-induced cytidine deaminase (AID) deficiency causes the autosomal recessive form of the Hyper-IgM syndrome (HIGM2). Cell. 2000; 102:565–575. [PubMed: 11007475]
10. Pham P, Bransteitter R, Petruska J, Goodman MF. Processive AID-catalysed cytosine deamination on single-stranded DNA simulates somatic hypermutation. Nature. 2003; 424:103–107. [PubMed: 12819663]
11. Yu K, Huang FT, Lieber MR. DNA substrate length and surrounding sequence affect the activation-induced deaminase activity at cytidine. J. Biol. Chem. 2004; 279:6496–6500. [PubMed: 14645244]
12. Neuberger MS, Harris RS, Di Noia J, Petersen-Mahrt SK. Immunity through DNA deamination. Trends Biochem. Sci. 2003; 28:305–312. [PubMed: 12826402]
13. Rada C, Di Noia JM, Neuberger MS. Mismatch recognition and uracil excision provide complementary paths to both Ig switching and the A/T-focused phase of somatic mutation. Mol. Cell. 2004; 16:163–171. [PubMed: 15494304]

Author Manuscript Author Manuscript Author Manuscript Author Manuscript

14. Bross L, Muramatsu M, Kinoshita K, Honjo T, Jacobs H. DNA double-strand breaks: prior to but not sufficient in targeting hypermutation. J. Exp. Med. 2002; 195:1187–1192. [PubMed: 11994423]
15. Papavasiliou FN, Schatz DG. The activation-induced deaminase functions in a postcleavage step of the somatic hypermutation process. J. Exp. Med. 2002; 195:1193–1198. [PubMed: 11994424]
16. Casali P, Zan H. Class switching and *myc* translocation: how does DNA break? Nat. Immunol. 2004; 5:1101–1103. [PubMed: 15496946]
17. Unniraman S, Zhou S, Schatz DG. Identification of an AID-inde-pendent pathway for chromosomal translocations between the IgH switch region and Myc. Nat. Immunol. 2004; 5:1117–1123. [PubMed: 15489857]
18. Rush JS, Fugmann SD, Schatz DG. Staggered AID-dependent DNA double strand breaks are the predominant DNA lesions targeted to Sm in Ig class switch recombination. Int. Immunol. 2004; 16:549–557. [PubMed: 15039385]
19. Schrader CE, Linehan EK, Mochegova SN, Woodland RT, Stavnezer J. Inducible DNA breaks in Ig S regions are dependent on AID and UNG. J. Exp. Med. 2005; 202:561–568. [PubMed: 16103411]
20. Buermeyer AB, Deschenes SM, Baker SM, Liskay RM. Mammalian DNA mismatch repair. Annu. Rev. Genet. 1999; 33:533–564. [PubMed: 10690417]
21. Edelmann L, Edelmann W. Loss of DNA mismatch repair function and cancer predisposition in the mouse: animal models for human hereditary nonpolyposis colorectal cancer. Am. J. Med. Genet. C Semin. Med. Genet. 2004; 129:91–99. [PubMed: 15264277]
22. Harfe BD, Jinks-Robertson S. DNA mismatch repair and genetic instability. Annu. Rev. Genet. 2000; 34:359–399. [PubMed: 11092832]
23. Jiricny J. Mediating mismatch repair. Nat. Genet. 2000; 24:6–8. [PubMed: 10615114]
24. Kunkel TA, Erie DA. DNA mismatch repair. Annu. Rev. Biochem. 2004; 22:681–710.
25. Diaz M, Casali P. Somatic immunoglobulin hypermutation. Curr. Opin. Immunol. 2002; 14:235–240. [PubMed: 11869898]
26. de Vries SS, Baart EB, Dekker M, Siezen A, de Rooij DG, de Boer P, te Riele H. Mouse MutS-like protein Msh5 is required for proper chromosome synapsis in male and female meiosis. Genes Dev. 1999; 13:523–531. [PubMed: 10072381]
27. Edelmann W, Cohen PE, Kneitz B, Winand N, Lia M, Heyer J, Kolodner R, Pollard JW, Kucherlapati R. Mammalian MutS ho-mologue 5 is required for chromosome pairing in meiosis. Nat. Genet. 1999; 21:123–127. [PubMed: 9916805]
28. Kong Q, Maizels N. PMS2-deficiency diminishes hypermutation of a λ1 transgene in young but not older mice. Mol. Immunol. 1999; 36:83–91. [PubMed: 10378680]
29. Kneitz B, Cohen PE, Avdievich E, Zhu L, Kane MF, Hou H, Kolodner RD Jr, Kucherlapati R, Pollard JW, Edelmann W. MutS ho-molog 4 localization to meiotic chromosomes is required for chromosome pairing during meiosis in male and female mice. Genes Dev. 2000; 14:1085–1097. [PubMed: 10809667]
30. Prolla TA, Baker SM, Harris AC, Tsao JL, Yao X, Bronner CE, Zheng B, Gordon M, Reneker J, Arnheim N, Shibata D, Bradley A, Liskay RM. Tumour susceptibility and spontaneous mutation in mice deficient in Mlh1, Pms1 and Pms2 DNA mismatch repair. Nat. Genet. 1998; 18:276–279. [PubMed: 9500552]
31. Ehrenstein MR, Neuberger MS. Deficiency in Msh2 affects the efficiency and local sequence specificity of immunoglobulin class-switch recombination: parallels with somatic hypermutation. EMBO J. 1999; 18:3484–3490. [PubMed: 10369687]
32. Schrader CE, Edelmann W, Kucherlapati R, Stavnezer J. Reduced isotype switching in splenic B cells from mice deficient in mismatch repair enzymes. J. Exp. Med. 1999; 190:323–330. [PubMed: 10430621]
33. Schrader CE, Vardo J, Stavnezer J. Role for mismatch repair proteins Msh2, Mlh1, and Pms2 in immunoglobulin class switching shown by sequence analysis of recombination junctions. J. Exp. Med. 2002; 195:367–373. [PubMed: 11828012]
34. Schrader CE, Vardo J, Stavnezer J. Mlh1 can function in antibody class switch recombination independently of Msh2. J. Exp. Med. 2003; 197:1377–1383. [PubMed: 12743174]

Author Manuscript Author Manuscript Author Manuscript Author Manuscript

35. Rada C, Ehrenstein MR, Neuberger MS, Milstein C. Hot spot focusing of somatic hypermutation in MSH2-deficient mice suggests two stages of mutational targeting. Immunity. 1998; 9:135–141. [PubMed: 9697843]
36. Phung QH, Winter DB, Cranston A, Tarone RE, Bohr VA, Fishel R, Gearhart PJ. Increased hypermutation at G and C nucleotides in immunoglobulin variable genes from mice deficient in the MSH2 mismatch repair protein. J. Exp. Med. 1998; 187:1745–1751. [PubMed: 9607916]
37. Delbos F, De Smet A, Faili A, Aoufouchi S, Weill JC, Reynaud CA. Contribution of DNA polymerase η to immunoglobulin gene hypermutation in the mouse. J. Exp. Med. 2005; 201:1191–1196. [PubMed: 15824086]
38. Li Z, Scherer SJ, Ronai D, Iglesias-Ussel MD, Peled JU, Bardwell PD, Zhuang M, Lee K, Martin A, Edelmann W, Scharff MD. Examination of Msh6- and Msh3-deficient mice in class switching reveals overlapping and distinct roles of MutS homologues in antibody diversification. J. Exp. Med. 2004; 200:47–59. [PubMed: 15238604]
39. Martomo SA, Yang WW, Gearhart PJ. A role for Msh6 but not Msh3 in somatic hypermutation and class switch recombination. J. Exp. Med. 2004; 200:61–68. [PubMed: 15238605]
40. Wiesendanger M, Kneitz B, Edelmann W, Scharff MD. Somatic hypermutation in MutS homologue (MSH) 3-, MSH6-, and MSH3/MSH6-deficient mice reveals a role for the MSH2-MSH6 heterodimer in modulating the base substitution pattern. J. Exp. Med. 2000; 191:579–584. [PubMed: 10662804]
41. Kim N, Bozek G, Lo JC, Storb U. Different mismatch repair deficiencies all have the same effects on somatic hypermutation: intact primary mechanism accompanied by secondary modifications. J. Exp. Med. 1999; 190:21–30. [PubMed: 10429667]
42. Phung QH, Winter DB, Alrefai R, Gearhart PJ. Hypermutation in Ig *V* genes from mice deficient in the MLH1 mismatch repair protein. J. Immunol. 1999; 162:3121–3124. [PubMed: 10092760]
43. Ehrenstein MR, Rada C, Jones AM, Milstein C, Neuberger MS. Switch junction sequences in PMS2-deficient mice reveal a microhomology-mediated mechanism of Ig class switch recombination. Proc. Natl. Acad. Sci. USA. 2001; 98:14553–14558. [PubMed: 11717399]
44. Winter DB, Phung QH, Umar A, Baker SM, Tarone RE, Tanaka K, Liskay RM, Kunkel TA, Bohr VA, Gearhart PJ. Altered spectra of hypermutation in antibodies from mice deficient for the DNA mismatch repair protein PMS2. Proc. Natl. Acad. Sci. USA. 1998; 95:6953–6958. [PubMed: 9618520]
45. Cascalho M, Wong J, Steinberg C, Wabl M. Mismatch repair co-opted by hypermutation. Science. 1998; 279:1207–1210. [PubMed: 9469811]
46. Frey S, B. B, Delbos F, Quint L, Weill JC, Reynaud CA. Mismatch repair deficiency interferes with the accumulation of mutations in chronically stimulated B cells and not with the hypermutation process. Immunity. 1998; 9:127–134. [PubMed: 9697842]
47. Martin A, Li Z, Lin DP, Bardwell PD, Iglesias-Ussel MD, Edelmann W, Scharff MD. Msh2 ATPase activity is essential for somatic hypermutation at A-T basepairs and for efficient class switch recombination. J. Exp. Med. 2003; 198:1171–1178. [PubMed: 14568978]
48. Larson ED, Duquette ML, Cummings WJ, Streiff RJ, Maizels N. MutSα binds to and promotes synapsis of transcriptionally activated immunoglobulin switch regions. Curr. Biol. 2005; 15:470–474. [PubMed: 15753043]
49. Wilson TM, Vaisman A, Martomo SA, Sullivan P, Lan L, Hanaoka F, Yasui A, Woodgate R, Gearhart PJ. MSH2-MSH6 stimulates DNA polymerase η, suggesting a role for A:T mutations in antibody genes. J. Exp. Med. 2005; 201:637–645. [PubMed: 15710654]
50. Lipkin SM, Wang V, Jacoby R, Banerjee-Basu S, Baxevanis AD, Lynch HT, Elliott RM, Collins FS. MLH3: a DNA mismatch repair gene associated with mammalian microsatellite instability. Nat. Genet. 2000; 24:27–35. [PubMed: 10615123]
51. Kondo E, Horii A, Fukushige S. The interacting domains of three MutL heterodimers in man: hMLH1 interacts with 36 homologous amino acid residues within hMLH3, hPMS1 andhPMS2. Nucleic Acids Res. 2001; 29:1695–1702. [PubMed: 11292842]
52. Lipkin SM, Moens PB, Wang V, Lenzi M, Shanmugarajah D, Gilgeous A, Thomas J, Cheng J, Touchman JW, Green ED, Schwartzberg P, Collins FS, Cohen PE. Meiotic arrest and aneuploidy in MLH3-deficient mice. Nat. Genet. 2002; 31:385–390. [PubMed: 12091911]

Author Manuscript Author Manuscript Author Manuscript Author Manuscript

53. McDonald JP, Frank EG, Plosky BS, Rogozin IB, Masutani C, Hanaoka F, Woodgate R, Gearhart PJ. 129-derived strains of mice are deficient in DNA polymerase ι and have normal immunoglobulin hypermutation. J. Exp. Med. 2003; 198:635–643. [PubMed: 12925679]
54. Jolly CJ, Klix N, Neuberger MS. Rapid methods for the analysis of immunoglobulin gene hypermutation: application to transgenic and gene targeted mice. Nucleic Acids Res. 1997; 25:1913–1919. [PubMed: 9115357]
55. Hodgkin PD, Lee JH, Lyons AB. B cell differentiation and isotype switching is related to division cycle number. J. Exp. Med. 1996; 184:277–281. [PubMed: 8691143]
56. Baker SM, Bronner CE, Zhang L, Plug AW, Robatzek M, Warren G, Elliott EA, Yu J, Ashley T, Arnheim N, Flavell RA, Liskay RM. Male mice defective in the DNA mismatch repair gene *PMS2* exhibit abnormal chromosome synapsis in meiosis. Cell. 1995; 82:309–319. [PubMed: 7628019]
57. de Wind N, Dekker M, Berns A, Radman M, te Riele H. In activation of the mouse *Msh2* gene results in mismatch repair deficiency methylation tolerance. Cell. 1995; 82:321–330. [PubMed: 7628020]
58. Reitmair AH, Schmits R, Ewel A, Bapat B, Redston M, Mitri A, Waterhouse A, Mittru¨cker HW, Wakeham A, Liu B, et al. MSH2 deficient mice are viable and susceptible to lymphoid tumours. Nat. Genet. 1995; 11:64–70. [PubMed: 7550317]
59. Baker SM, Plug AW, Prolla TA, Bronner CE, Harris AC, Yao X, Christie DM, Monell C, Arnheim N, Bradley A, Ashley T, Liskay RM. Involvement of mouse Mlh1 in DNA mismatch repair and meiotic crossing over. Nat. Genet. 1996; 13:336–342. [PubMed: 8673133]
60. Edelmann W, Cohen PE, Kane M, Lau K, Morrow B, Bennett S, Umar A, Kunkel T, Cattoretti G, Chaganti R, Pollard JW, Kolodner RD, Kucherlapati R. Meiotic pachytene arrest in MLH1-deficient mice. Cell. 1996; 85:1125–1134. [PubMed: 8674118]
61. Edelmann W, Yang K, Umar A, Heyer J, Lau K, Fan K, Liedtke W, Cohen PE, Kane MF, Lipford JR, et al. Mutation in the mismatch repair gene Msh6 causes cancer susceptibility. Cell. 1997; 91:467–477. [PubMed: 9390556]
62. Chen J, Kuriaguchi M, Reichow D, Dudley S, Arnheim N, Liskay RM, Lipkin MS. Contributions by MutL homologs Mlh3 and Pms2 to DNA mismatch repair and tumor suppression in the mouse. Cancer Res. 2005; 65:8662–8670. [PubMed: 16204034]
63. Flores-Rozas H, Kolodner RD. The *Saccharomyces cerevisiae MLH3* gene functions in MSH3-dependent suppression of frameshift mutations. Proc. Natl. Acad. Sci. USA. 1998; 95:12404–12409. [PubMed: 9770499]
64. Pan Q, Petit-Frere C, Lahdesmaki A, Gregorek H, Chrzanowska KH, Hammarstrom L. Alternative end joining during switch recombination in patients with ataxia-telangiectasia. Eur. J. Immunol. 2002; 32:1300–1308. [PubMed: 11981817]
65. Lahdesmaki A, Taylor AM, Chrzanowska KH, Pan-Hammarstrom Q. Delineation of the role of the Mre11 complex in class switch recombination. J. Biol. Chem. 2004; 279:16479–16487. [PubMed: 14747472]
66. Lumsden JM, McCarty T, Petiniot LK, Shen R, Barlow C, Wynn TA, Morse HCr, Gearhart PJ, Wynshaw-Boris A, Max EE, Hodes RJ. Immunoglobulin class switch recombination is impaired in Atm-deficient mice. J. Exp. Med. 2004; 200:1111–1121. [PubMed: 15504820]
67. Reina-San-Martin B, Chen HT, Nussenzweig A, Nussenzweig MC. ATM is required for efficient recombination between immunoglobulin switch regions. J. Exp. Med. 2004; 200:1103–1110. [PubMed: 15520243]
68. Min IM, Schrader CE, Vardo J, Luby TM, D'Avirro N, Stavnezer J, Selsing E. The Sm tandem repeat region is critical for Ig isotype switching in the absence of Msh2. Immunity. 2003; 19:515–524. [PubMed: 14563316]
69. Min IM, Rothlein LR, Schrader CE, Stavnezer J, Selsing E. Shifts in targeting of class switch recombination sites in mice that lack m switch region tandem repeats or Msh2. J. Exp. Med. 2005; 201:1885–1890. [PubMed: 15955838]
70. Zarrin AA, Alt FW, Chaudhuri J, Stokes N, Kaushal D, Du Pasquier L, Tian M. An evolutionarily conserved target motif for immunoglobulin class-switch recombination. Nat. Immunol. 2004; 5:1275–1281. [PubMed: 15531884]

Author Manuscript Author Manuscript Author Manuscript Author Manuscript

71. Bardwell PD, Woo CJ, Wei K, Li Z, Martin A, Z. SS, Parris T, Edelmann W, Scharff MD. Altered somatic hypermutation and reduced class-switch recombination in exonuclease 1-mutant mice. Nat. Immunol. 2004; 5:224–229. [PubMed: 14716311]

72. Rogozin IB, Pavlov YI, Bebenek K, Matsuda T, Kunkel TA. Somatic mutation hotspots correlate with DNA polymerase η error spectrum. Nat. Immunol. 2001; 2:530–536. [PubMed: 11376340]

73. Zeng X, Winter DB, Kasmer C, Kraemer KH, Lehmann AR, Gearhart PJ. DNA polymerase η is an A-T mutator in somatic hypermutation of immunoglobulin variable genes. Nat. Immunol. 2001; 2:537–541. [PubMed: 11376341]

74. Pavlov YI, Rogozin IB, Galkin AP, Aksenova AY, Hanaoka F, Rada C, Kunkel TA. Correlation of somatic hypermutation specificity and A-T base pair substitution errors by DNA polymerase eta during copying of a mouse immunoglobulin κ light chain transgene. Proc. Natl. Acad. Sci. USA. 2002; 99:9954–9959. [PubMed: 12119399]

75. Faili A, Aoufouchi S, Flatter E, Gueranger Q, Reynaud CA, Weill JC. Induction of somatic hypermutation in immunoglobulin genes is dependent on DNA polymerase iota. Nature. 2002; 419:944–947. [PubMed: 12410315]

76. Zan H, Zhong Y, Xu Z, Evinger AJ, Shima N, Schimenti JC, Casali P. The translesion DNA polymerase θ plays a dominant role in immunoglobulin gene somatic hypermutation. EMBO J. 2005; 24:3757–3769. [PubMed: 16222339]

77. Zan H, Komori A, Li Z, Cerutti A, Schaffer A, Flajnik MF, Diaz M, Casali P. The translesion DNA polymerase ζ plays a major role in Ig and *bcl-6* somatic hypermutation. Immunity. 2001; 14:643–653. [PubMed: 11371365]

Author Manuscript Author Manuscript Author Manuscript Author Manuscript

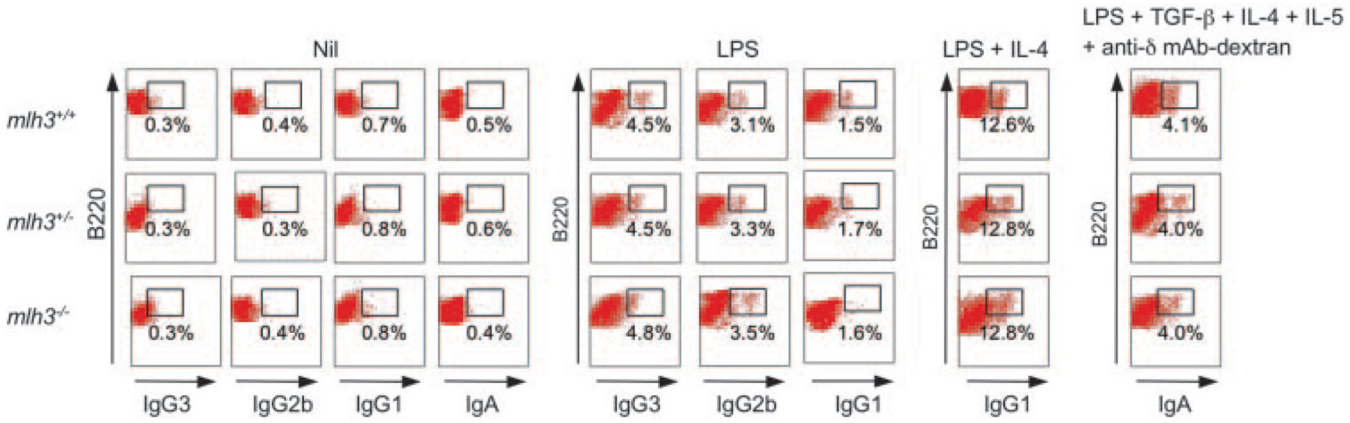

FIGURE 1.

CSR in B cells from 129 Sv/Ev mice, as assessed by detection of surface IgG3, IgG2b, IgG1, and IgA on in vitro-stimulated B cells. B cells were isolated from 8- to 12-wk-old *mlh3*$^{+/+}$, mlh3$^{+/-}$ and *mlh3*$^{-/-}$ littermates and cultured in the absence (nil) or presence of LPS, LPS plus IL-4, or LPS plus TGF-β plus IL-5 plus IL-4 plus anti-δ mAb-dextran to induce CSR to IgG3 and IgG2b, IgG1 and IgA, respectively. Cells were collected 5 days after stimulation and stained with FITC-conjugated anti-mouse IgG3, IgG1, IgG2b, and IgA mAbs and PE-conjugated anti-mouse B220 mAb. Small boxed areas outline B220^{+}IgG^{+} or B220^{+}IgA^{+} cells.

Author Manuscript Author Manuscript Author Manuscript Author Manuscript

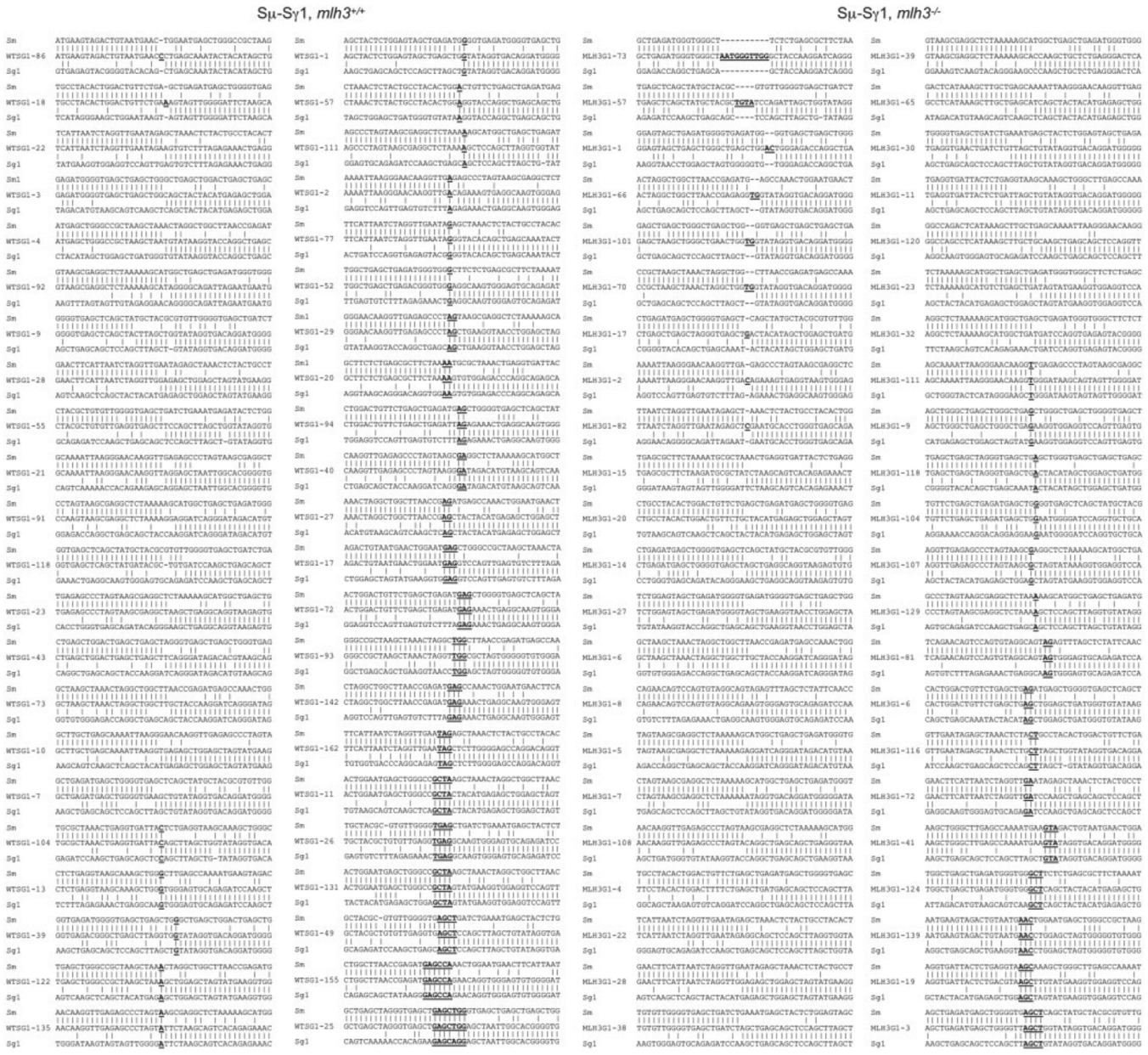

FIGURE 2.

Altered Sμ-Sγ1 DNA junctions in *mlh3*$^{-/-}$ B cells. B cells from *mlh3*$^{+/+}$ and *mlh3*$^{-/-}$ mice were stimulated by LPS and IL-4 in vitro for 5 days. Junctional Sμ-Sγ1 DNAs from stimulated cells were amplified, cloned, and sequenced. Each sequence is compared with the corresponding germline Sμ (MUSIGCD07) or Sγ1 sequence (MUSIGHANB). Microhomologies and insertions are in bold and underlined. Sequences were derived from stimulated B cells of 5 *mlh3*$^{+/+}$ and 5 *mlh3*$^{-/-}$ mice.

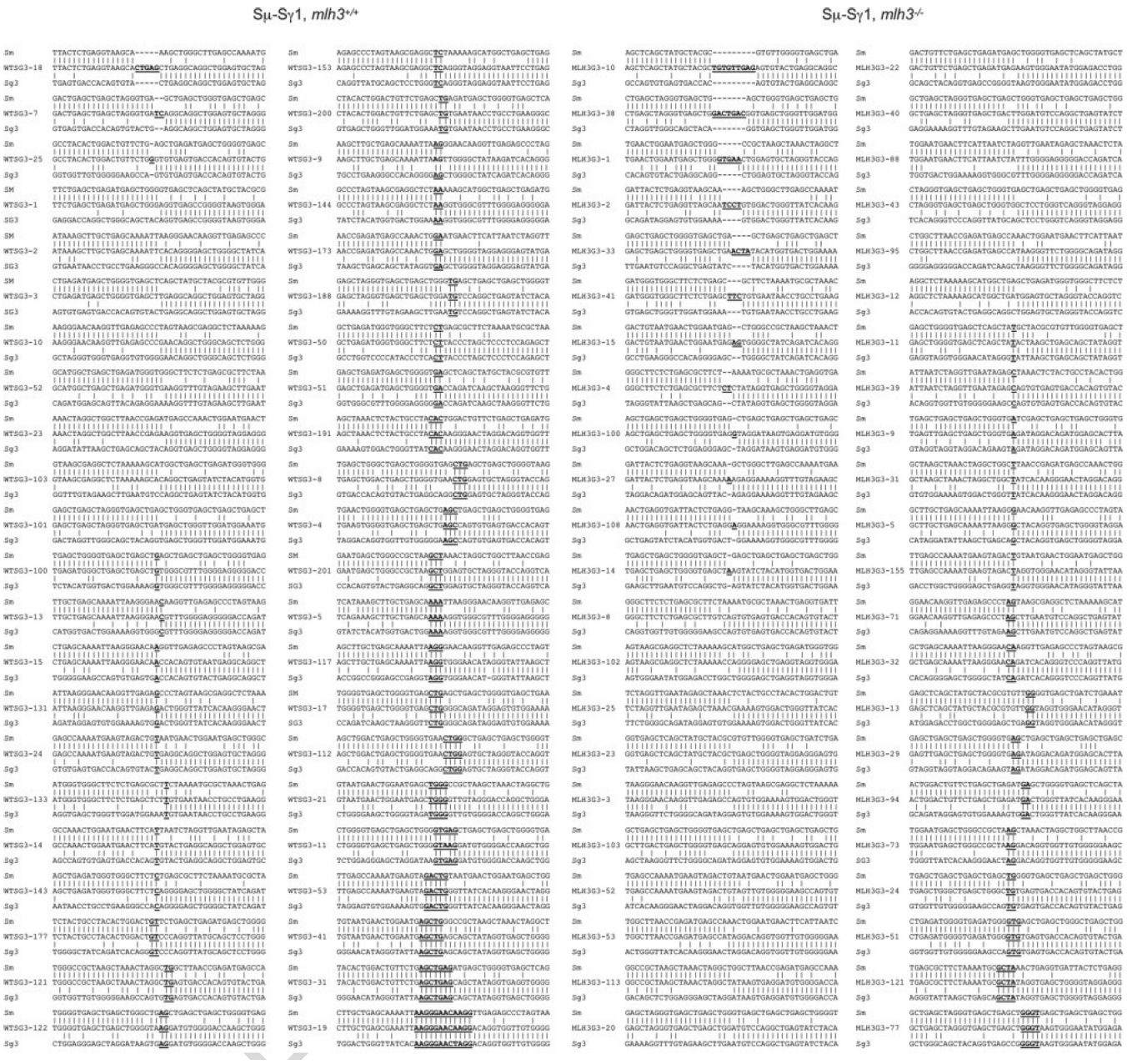

FIGURE 3.

Altered Sμ-Sγ3 DNA junctions in *mlh3*$^{-/-}$ B cells. B cells from *mlh3*$^{+/+}$ and *mlh3*$^{-/-}$ mice were stimulated by LPS in vitro for 5 days. Junctional Sμ-Sγ3 DNA was amplified, cloned, sequenced, and compared with the corresponding germline Sμ (MUSIGCD07) and Sγ3 region sequence (MUSIGCD18 or MUSIGHANA). Microhomologies and insertions are in bold and underlined. Sequences were derived from stimulated B cells of 5 *mlh3*$^{+/+}$ and 5 *mlh3*$^{-/-}$ mice.

Author Manuscript Author Manuscript Author Manuscript Author Manuscript

Author Manuscript Author Manuscript Author Manuscript Author Manuscript

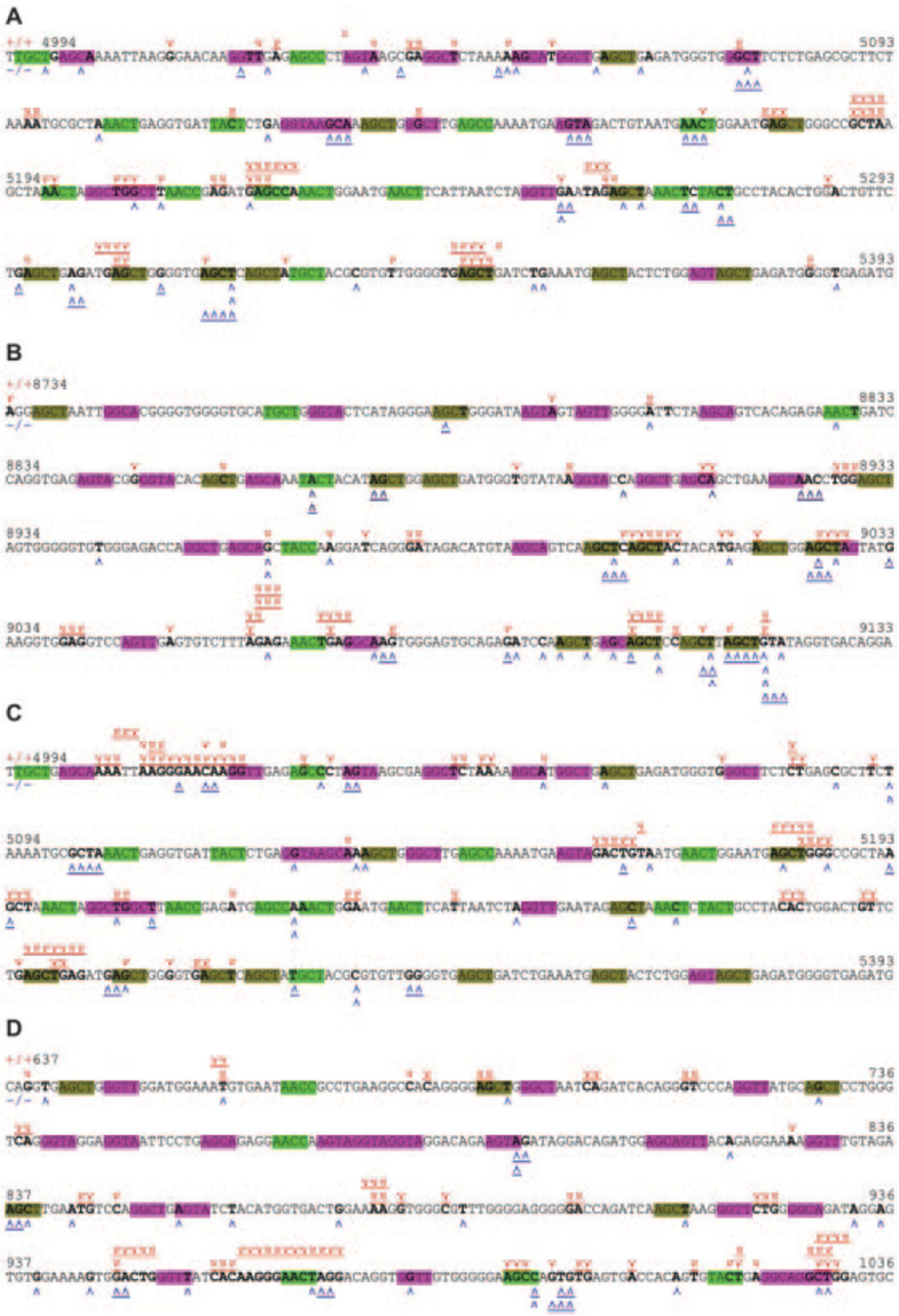

FIGURE 4.

DNA breakpoints in Sμ, Sγ1, and Sγ3 regions of junctional Sμ-Sγ1 and Sμ-Sγ3 DNA in *mlh3*$^{+/+}$ and *mlh3*$^{-/-}$ B cells. Sequences analyzed are identical to those analyzed in Figs. 2 and 3. Breakpoints are indicated by carets. The Sμ or Sγ breakpoints in *mlh3*$^{+/+}$ B cells are in red and above the sequence, and those in *mlh3*$^{-/-}$ B cells are in blue and below the sequence. Donor-acceptor microhomologies are indicated by underscored carets. More than 90% of Sμ breakpoints are located within 400 bp of Sμ DNA (MUSIGCD07 4994–5393), >92% Sγ1 breakpoints are within 400 bp of Sγ1 region (MUSIGHANB 8734–9133), and

Author Manuscript Author Manuscript Author Manuscript Author Manuscript

>75% Sγ3 breakpoints are within 400 bp of Sγ3 region (MUSIGCD18 637–1036) as shown here. RGYW, WRCY, and AGCT are in purple, green, and brown, respectively. Nucleotides at which breakpoints occurred are in bold. *A*, Breakpoints in Sμ of Sμ-Sγ1 junctions; *B*, breakpoints in Sγ1 of Sμ-Sγ1 junctions; *C*, breakpoints in Sμ of Sμ-Sγ3 junctions; *D*, breakpoints in Sγ3 of Sμ-Sγ3 junctions.

Author Manuscript Author Manuscript Author Manuscript Author Manuscript

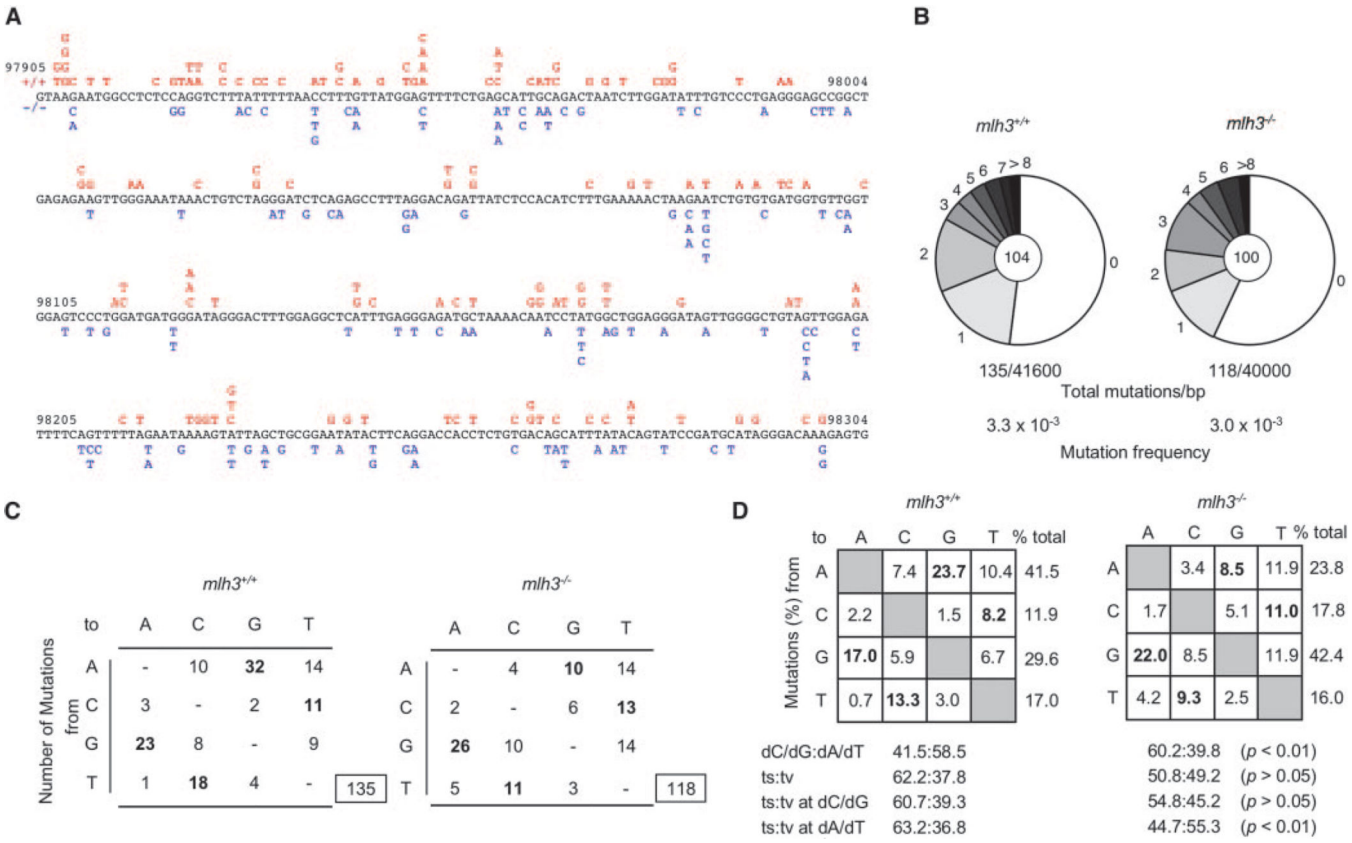

FIGURE 5.

Somatic mutations in the intronic DNA downstream of the rearranged $V_HJ558DJ_H4$ gene (J_H4 intronic DNA) in Peyer's patches B cells. *A*, J_H4 intronic DNA was amplified from germinal center $B220^+PNA^{high}$ B cells sorted from Peyer's patches of $mlh3^{+/+}$ and $mlh3^{-/-}$ mice. The sequence depicted spans 400 bp of intronic DNA downstream of J_H4 (AJ851868.1 97905–98304). Mutations in $mlh3^{+/+}$ are depicted above the sequence and those in$mlh3^{-/-}$ below. *B*, Pie charts of the proportions of sequences that carry 1, 2, 3, etc. mutations over the 400 bp of J_H4 intronic DNA analyzed. The numbers of the sequences analyzed are at the center of the pies. *C*, Numbers and nature of independent mutational events scored. *D*, Compilations with the numbers indicating percentages of all mutations scored in the pool of the target sequences of *A* and *B*. Below the compilations, the ratio of mutations at dC/dG to those at dA/dT is indicated, as is the ratio of transition-transversion substitutions at both dC/dG and dA/dT. Data are from 3 $mlh3^{+/+}$ and 3 $mlh3^{-/-}$ mice.

Author Manuscript Author Manuscript Author Manuscript Author Manuscript

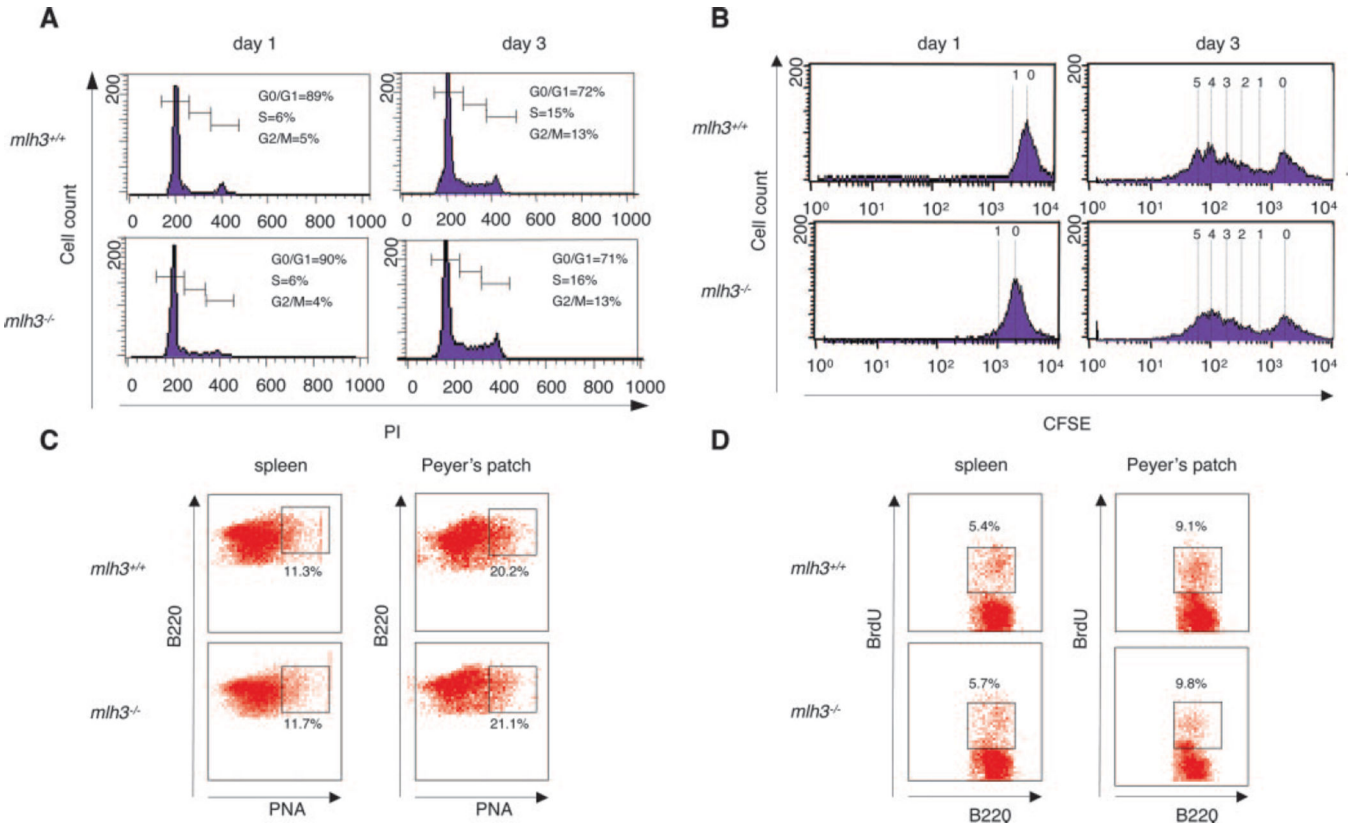

FIGURE 6.

Cell cycle and proliferation analysis. *A*, Cell cycle of *mlh3*$^{+/+}$ and *mlh3*$^{-/-}$ B cells in response to LPS stimulation as assessed by PI staining; *B*, cell proliferation of *mlh3*$^{+/+}$ and *mlh3*$^{-/-}$ B cells in response to LPS stimulation as assessed by CFSE staining; *C*, proportions of germinal center B220^{+}PNA^{high} B cells in *mlh3*$^{+/+}$ and *mlh3*$^{-/-}$ mice; *D*, in vivo proliferation of *mlh3*$^{+/+}$ and *mlh3*$^{-/-}$ B cells as assessed by BrdU incorporation.

Author Manuscript Author Manuscript Author Manuscript Author Manuscript

J Immunol. Author manuscript; available in PMC 2015 October 27.

Table I

Impact of deficiencies of MMR proteins on CSR and SHM

	CSR		SHM				
			Frequency		Pattern of substitutions		
MMR Protein Deficiency	**Efficacy**	**S-S microhomologies**	**In J_H4 intron**	**RGYW/WRCY targeting**	**dC/dG:dA/dT**	**ts:tv @ dC/dG**	**ts:tv @ dA/dT**
MutS homologs							
Msh2	↓ [a] (31, 32)[b]	↓ (33, 34)	↓ (35)	↑ (35)	↑ (13, 35, 36)	↑ (13, 37)	= (13, 37)
Msh3	= (38, 39)	= (38)	= (40)	= (40)	= (39, 40)	= (40)	= (40)
Msh4	Functions specifically during meiosis (26, 27, 29)						
Msh5	Functions specifically during meiosis (26, 27, 29)						
Msh6	↓ (38, 39)	= (38)	↓ (40)	↑ (39, 40)	↑ (38–40)	↑ (39, 40)	↓ (38)
MutL homologs							
Mlh1	↓ (32)	↑ (33, 34)	↓ (41, 42) in VDJ	Undetermined	↑ (41) or = (42)	= (42)	= (42)
Pms1	Functions only marginally in MMR30						
Pms2	↓ (32, 43)	↑ (32, 43)	↓ (41, 44, 46) in VDJ, = (43)	Undetermined	↑ (41) = (42, 43, 46)	= (42, 43, 46)	= (42, 43, 46)
MutS or MutL double knockout							
Msh3/Msh6	Undetermined	Undetermined	↓ (40)	↑ (40)	↑ (40)	↑ (40)	= (40)
Msh2/Mlh1	↓ (34)	↑ (34)	Undetermined	Undetermined	Undetermined	Undetermined	Undetermined

[a] ↑, increase; ↓, decrease; =, no change; ts, transition; tv, transversion.

[b] Numbers in parentheses are reference citations.

Author Manuscript Author Manuscript Author Manuscript Author Manuscript

Table II

Sμ-Sγ1 and Sμ-Sγ3 junctions in stimulated mlh3$^{+/+}$ and mlh3$^{-/-}$ B cells[a]

Mice	No. of Sequences Analyzed	Overlapping Junctions (microhomologies, no insertions)					Blunt Junctions (no microhomology, no insertions)	Nonoverlapping Junctions (no microhomologies, insertions)		
		1 nt	2 nt	3 nt	4 nt	≥5 nt	0 nt	1 nt	2 nt	≥3 nt
Sμ-Sγ1 junctions										
mlh3$^{+/+}$	44	11	5	5	4	2	15	2	0	0
mlh3$^{-/-}$	44	6	4	4	1	0	20	3	4	2
Sμ-Sγ3 junctions										
mlh3$^{+/+}$	44	8	11	7	2	5	8	1	1	1
mlh3$^{-/-}$	44	6	7	1	2	0	16	4	3	5

[a]Microhomologies (≥1–5 nt) in Sμ-Sγ1 ($p < 0.033$) and Sμ-Sγ3 ($p < 0.034$) junctions are less in *mlh3*$^{-/-}$ than in *mlh3*$^{+/+}$ B cells. Conversely, blunt junctions and insertions are more in *mlh3*$^{-/-}$ than in *mlh3*$^{+/+}$ B cells ($p < 0.048$ and $p < 0.016$ in Sμ-Sγ1 and Sμ-Sγ3 junctions, respectively).

Author Manuscript Author Manuscript Author Manuscript Author Manuscript

Table III

Locations of Sμ, Sγ1, and Sγ3 breakpoints in junctional Sμ-Sγ1 and Sμ-Sγ3 DNA sequences[a]

	Sμ Breakpoints in Sμ-Sγ1		**Sγ1 breakpoints in Sμ-Sγ3**	
Mice	**Within RGYW/ WRCY[b] (220 nt)**	**Outside RGYW/ WRCY (280 nt)**	**Within RGYW/ WRCY (180 nt)**	**Outside RGYW/ WRCY (320 nt)**
mlh3$^{+/+}$	26 (59)	18 (41)	15 (34)	29 (66)
mlh3$^{-/-}$	24 (55)	20 (45)	25 (57)	19 (43)
	Sμ breakpoints in Sμ-Sγ1		Sγ3 breakpoints in Sμ-Sγ3	
Mice	Within RGYW/ WRCY (220 nt)	Outside RGYW/ WRCY (280 nt)	Within RGYW/ WRCY (210 nt)	Outside RGYW/ WRCY (290 nt)
mlh3$^{+/+}$	22 (50)	22 (50)	13 (30)	31 (70)
mlh3$^{-/-}$	19 (43)	25 (57)	24 (55)	20 (45)

[a] Numbers in parentheses following RGYW/WRCY are nt residues comprising (within) or noncomprising (outside) the indicated motifs of a total of 500 nt (length of the S region segment). Numbers in parentheses following each datum are percentages of the targeting of breakpoints within or outside RGYW/WRCY. Sγ1 and Sγ3 breakpoints preferentially target RGYW/WRCY in *mlh3*$^{-/-}$ B cells ($p < 0.05$). Targeting of RGYW/WRCY by Sμ breakpoints in either Sμ-Sγ1 or Sμ-Sγ3 junctions is not different in *mlh3*$^{-/-}$ and *mlh3*$^{+/+}$ B cells ($p > 0.05$).

[b] RGYW/WRCY contains the AID hotspot WRC/GYW, which was also preferentially targeted by Sγ1 and Sγ3 region breakpoints in *mlh3*$^{-/-}$ B cells.

Author Manuscript Author Manuscript Author Manuscript Author Manuscript

Table IV

Distributions of Sμ, Sγ1, and *S*γ3 breakpoints entailing microhomologies (overlapping, ≥1 nt) and no-microhomologies (nonoverlapping, blunt junctions and insertions) in junctional Sμ-Sγ1 and Sμ-Sγ3 sequences[a]

	Sμ Breakpoints in Sμ-Sγ1				**Sγ1 Breakpoints in Sμ-Sγ1**			
	Within RGYW/WRCY[b]		**Outside RGYW/WRCY**		**Within RGYW/WRCY**		**Outside RGYW/WRCY**	
Mice	**Overlapping**	**Nonoverlapping**	**Overlapping**	**Nonoverlapping**	**Overlapping**	**Nonoverlapping**	**Overlapping**	**Nonoverlapping**
mlh3$^{+/+}$	15 (58)	11 (42)	12 (67)	6 (33)	11 (73)	4 (27)	16 (55)	13 (45)
mlh3$^{-/-}$	10 (42)	14 (58)	5 (25)	15 (75)	11 (44)	14 (56)	4 (21)	15 (79)
	Sμ Breakpoints in Sμ-Sγ3				Sγ3 Breakpoints in Sμ-Sγ3			
	Within RGYW/WRCY		Outside RGYW/WRCY		Within RGYW/WRCY		Outside RGYW/WRCY	
Mice	Overlapping	Nonoverlapping	Overlapping	Nonoverlapping	Overlapping	Nonoverlapping	Overlapping	Nonoverlapping
mlh3$^{+/+}$	17 (77)	5 (23)	16 (73)	6 (27)	11 (85)	2 (15)	22 (71)	9 (29)
mlh3$^{-/-}$	7 (37)	12 (63)	9 (36)	16 (64)	11 (46)	13 (54)	5 (25)	15 (75)

[a] Numbers in parentheses are percentages of the targeting of breakpoints entailing microhomologies (overlapping) and no-microhomologies (nonoverlapping) within or outside RGYW/WRCY, respectively. Distributions of Sμ, Sγ1, and Sγ3 breakpoints entailing microhomologies and nonmicrohomologies in Sμ-Sγ1 and Sμ-Sγ3 junctional sequences are altered in *mlh3*$^{-/-}$ B cells ($p < 0.01$). In Sμ-Sγ1 and Sμ-Sγ3 junctions not involving microhomologies, targeting of Sγ1 and Sγ3 breakpoints to nucleotide residues within RGYW/WRCY or WRC/GYW increased in *mlh3*$^{-/-}$ B cells compared with *mlh3*$^{+/+}$ B cells. Conversely, in Sμ-Sγ1 and Sμ-Sγ3 junctions involving microhomologies, targeting of Sγ1 and Sγ3 breakpoints to nucleotide residues outside RGYW/WRCY or WRC/GYW decreased in *mlh3*$^{-/-}$ B cells compared with *mlh3*$^{+/+}$ B cells.

[b] RGYW/WRCY contains the AID hotspot WRC/GYW.

Author Manuscript

Author Manuscript

Author Manuscript

Author Manuscript

Table V

Distributions of somatic mutations within and outside RGYW/WRCY[a]

	Mutations at dC/dG		Mutations at dA/dT	
Mice	**Within RGYW/WRCY[b] (84 nt)**	**Outside RGYW/WRCY (316 nt)**	**Within RGYW/WRCY (84 nt)**	**Outside RGYW/WRCY (316 nt)**
mlh3$^{+/+}$	15 (28)	39 (72)	12 (15)	69 (85)
mlh3$^{-/-}$	33 (46)	39 (54)	9 (20)	37 (80)

[a] Mutations at dC/dG preferentially targeted RGYW/WRCY in *mlh3*$^{-/-}$ mice as compared with *mlh3*$^{+/+}$ mice ($p < 0.05$). Numbers in parenthesis following RGYW/WRCY are nucleotide (nt) residues comprising (within) or uncomprising (outside) RGYW/WRCY motif of a total of 400 nt (length of the J_H4 intronic DNA segment). Numbers in parentheses following each datum are the percentages of mutations targeting RGYW/WRCY or other nucleotides.

[b] RGYW/WRCY contains the AID hotspot WRC/GYW, which was also preferentially targeted by mutations at dC/dG in *mlh3*$^{-/-}$ mice.